THE ROYAL SOCIETY

Published online 3 October 2002

Water oxidation chemistry of photosystem II

John S. Vrettos and Gary W. Brudvig*

Department of Chemistry, Yale University, PO Box 208107, New Haven, CT 06520-8107, USA

The O_2-evolving complex of photosystem II catalyses the light-driven four-electron oxidation of water to dioxygen in photosynthesis. In this article, the steps leading to photosynthetic O_2 evolution are discussed. Emphasis is given to the proton-coupled electron-transfer steps involved in oxidation of the manganese cluster by oxidized tyrosine Z ($Y_Z^{\cdot}$), the function of Ca^{2+} and the mechanism by which water is activated for formation of an O–O bond. Based on a consideration of the biophysical studies of photosystem II and inorganic manganese model chemistry, a mechanism for photosynthetic O_2 evolution is presented in which the O–O bond-forming step occurs via nucleophilic attack on an electron-deficient Mn^{V}=O species by a calcium-bound water molecule. The proposed mechanism includes specific roles for the tetranuclear manganese cluster, calcium, chloride, Y_Z and His190 of the D1 polypeptide. Recent studies of the ion selectivity of the calcium site in the O_2-evolving complex and of a functional inorganic manganese model system that test key aspects of this mechanism are also discussed.

Keywords: calcium; chloride; manganese; oxygen-evolving complex; photosystem II; tyrosyl radical

1. PHOTOSYSTEM II AND THE OXYGEN-EVOLVING COMPLEX

Photosynthetic O_2 production is catalysed by PSII, a transmembrane complex of proteins found in the thylakoid membrane of plants and cyanobacteria. The core D1 and D2 subunits of PSII form a heterodimer that contains the redox centres which couple the reduction of plastoquinone to the oxidation of water. A crystal structure for the PSII complex has been solved at 3.8 Å resolution (Zouni *et al.* 2001). In this structure, the positions of the transmembrane α-helices can be determined, but the positions of loop regions, individual amino acids and the ligands to metal cofactors cannot be discerned. Before the recent determination of the X-ray crystal structure, structural studies of PSII had relied on analogy to the homologous bacterial photosynthetic reaction centre, the high-resolution structure of which is known (Michel & Deisenhofer 1988).

The energy required to oxidize water to O_2 is provided by visible photons, which are collected by an array of chlorophylls in light-harvesting proteins and funnelled by energy-transfer mechanisms to the photoactive reaction-centre chlorophyll in PSII (P_{680}). The excited state of P_{680} is a strong reductant that transfers an electron to a pheophytin molecule, which in turn reduces the protein-bound plastoquinone electron acceptor in PSII (Q_A). The final electron acceptor is a diffusible plastoquinone (Q_B). Following its reduction to hydroquinone, Q_BH_2 dissociates from PSII and carries its reducing equivalents on to the next step in photosynthesis.

* Author for correspondence (gary.brudvig@yale.edu).

One contribution of 21 to a Discussion Meeting Issue 'Photosystem II: molecular structure and function'.

The charge-separated state $P_{680}^{+\cdot}/Q_A^{-\cdot}$ is stabilized through reduction of $P_{680}^{+\cdot}$ by a redox-active tyrosine residue, Y_Z. The tyrosyl radical thus formed, $Y_Z^{\cdot}$, oxidizes a tetranuclear manganese-oxo (Mn_4) cluster, the active site of water oxidation. Each oxidation state of the Mn_4 cluster is referred to as an S_n state ($n = 0-4$). S_0 is the most reduced and S_4 is the most oxidized of the S states formed during the four-electron cycle leading to O_2 evolution (Kok *et al.* 1970; Joliot & Kok 1975). Upon oxidation to the S_4 state, the Mn_4 cluster is spontaneously reduced to S_0 by oxidizing water to form O_2 and protons (Debus 1992; Rutherford *et al.* 1992; Yachandra *et al.* 1996; Vrettos *et al.* 2001*a*). Calcium and chloride are required for advancement beyond the S_2 state (Ghanotakis *et al.* 1984; Ono & Inoue 1984; Boussac *et al.* 1989; Andréasson *et al.* 1995; Wincencjusz *et al.* 1997). Together, Y_Z, the Mn_4 cluster, Ca^{2+} and Cl^- constitute the OEC. Several amino acids have been shown to affect the functionality of the OEC. They are thought to be either ligands to the Mn_4 cluster, such as D170 (Nixon & Diner 1992; Chu *et al.* 1995*a*) and H332 (Chu *et al.* 1995*b*; Debus *et al.* 2000), or participants in proton-coupled electron-transfer reactions, such as H190 (Chu *et al.* 1995*a*; Hays *et al.* 1998, 1999; Mamedov *et al.* 1998).

2. PROTON-COUPLED ELECTRON-TRANSFER REACTIONS AND S-STATE ADVANCEMENT

The oxidation of Y_Z by $P_{680}^{+\cdot}$, in both the presence and absence of the Mn_4 cluster, results in $Y_Z^{\cdot}$, which is a neutral radical (Tommos *et al.* 1995). Based on evidence that the pK_a of the hydroxyl group of Y_Z is greater than 9 (Hays *et al.* 1999), the reduced form of Y_Z is expected to be protonated over the physiological range of pH (Berthomieu *et al.* 1998). Consequently, a proton must be transferred from Y_Z to a nearby base during the photooxidation of Y_Z and from a nearby base to $Y_Z^{\cdot}$ during the

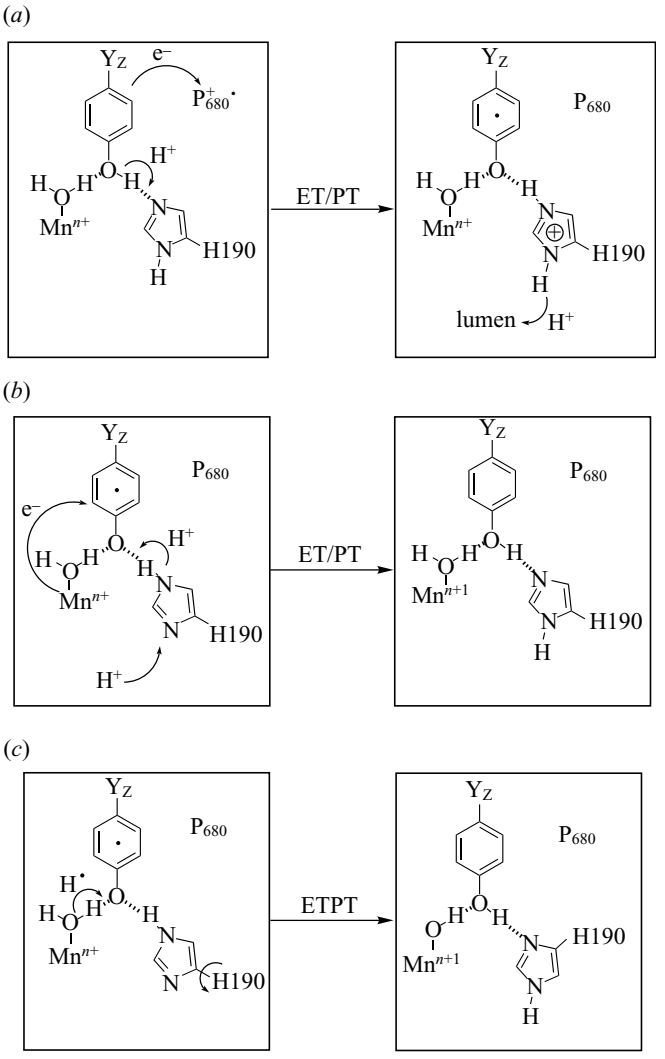

Figure 1. Models for PCET involved in (*a*) the photooxidation of Y_Z and (*b*,*c*) the subsequent reduction of $Y_Z^{\cdot}$. In the consecutive PCET mechanism (*b*), electrons and protons are transferred to separate sites (ET/PT). In the concerted PCET mechanism (*c*) for reduction of $Y_Z^{\cdot}$, both an electron and a proton are transferred from the Mn cluster to $Y_Z^{\cdot}$, resulting in an effective H-atom transfer (ETPT).

reduction of $Y_Z^{\cdot}$ (figure 1). Indeed, a substantial body of data provides evidence that both the photooxidation of Y_Z and the reduction of $Y_Z^{\cdot}$ involve the coupled transfer of an electron and a proton (Karge *et al.* 1997; Diner *et al.* 1998; Hays *et al.* 1998; Christen & Renger 1999; Christen *et al.* 1999; Hays *et al.* 1999; Kühne & Brudvig 2002).

In untreated PSII samples, electron transfer to and from Y_Z is very fast, but these events are retarded in PSII depleted of the Mn_4 cluster. These observations suggest that the Mn_4 cluster aids in ordering the H-bonding environment of the OEC to facilitate PCET during Y_Z oxidation and reduction (Tang *et al.* 1996*b*; Noguchi *et al.* 1997).

In Mn-depleted PSII, the rates for the oxidation and reduction of Y_Z are pH dependent and exhibit kinetic deuterium isotope effects (Rappaport & Lavergne 1997; Diner *et al.* 1998; Christen *et al.* 1999). The rate of Y_Z oxidation increases as the pH is raised and becomes extremely rapid as it approaches pH 9. The measured pK_a values of 8–10 and 5–7 (Mamedov *et al.* 1998; Hays *et al.* 1999) have been assigned, respectively, to those of Y_Z and its proton acceptor, which is thought to be H190. Thus, at a pH greater than 9, Y_Z is deprotonated and so its oxidation is no longer proton-limited and occurs most rapidly. Furthermore, the value of k_H/k_D is only slightly greater than 1 under these conditions (Diner *et al.* 1998). At pH values between 5 and 9, Y_Z oxidation is proton-coupled and proceeds normally, with k_H/k_D *ca.* 2.5–3.5. At a pH of less than 5, however, both Y_Z and its proton acceptor are protonated and so Y_Z oxidation is limited by proton transfer.

The identification of H190 as the proton acceptor to Y_Z is supported by site-directed mutagenesis experiments (Hays *et al.* 1998, 1999). Y_Z oxidation in H190 mutants occurs only at high pH, when Y_Z is deprotonated (Mamedov *et al.* 1998; Hays *et al.* 1999). The rate of Y_Z oxidation in H190 mutants at lower pH is improved by the addition of small organic bases, such as imidazole (Hays *et al.* 1998), which presumably act as proton acceptors and thereby rescue the proton-coupled steps. In contrast to Y_Z oxidation, the rate of $Y_Z^{\cdot}$ reduction has a less pronounced k_H/k_D of 1.4–2.3 (Diner *et al.* 1998) and neither the measured rates nor the H/D effect correlate with pH. This implies that, in the absence of the Mn_4 cluster, the reduction of $Y_Z^{\cdot}$ is not proton limited, either because the tyrosinate anion Y_Z^{-} is formed (at high pH) or because protons are readily available from solution (at low pH).

In contrast to Mn-depleted samples, the rates of oxidation of Y_Z in Mn-containing PSII are insensitive to H/D effects, consistent with a well-ordered pathway for PCET (Haumann *et al.* 1997; Karge *et al.* 1997; Christen & Renger 1999; Christen *et al.* 1999). However, k_H/k_D for the reduction of $Y_Z^{\cdot}$ during S-state advancement varies with S state (Bögershausen *et al.* 1996; Haumann *et al.* 1997; Karge *et al.* 1997). The reported values are 1.4 ($S_1 \rightarrow S_2$), 2.3 ($S_2 \rightarrow S_3$), 1.5 ($S_3 \rightarrow S_0$) and 1.4 ($S_0 \rightarrow S_1$). Similarly, the activation energies of the S-state transitions vary considerably and have been measured to be 59.4 kJ mol^{-1} ($S_0 \rightarrow S_1$), 9.6 kJ mol^{-1} ($S_1 \rightarrow S_2$) and 26.8 kJ mol^{-1} ($S_2 \rightarrow S_3$) (Koike *et al.* 1987). As might be expected from these results, only the $S_1 \rightarrow S_2$ transition can occur at low temperature (140 K) (Casey & Sauer 1984), whereas the other S-state advancements require temperatures above 220 K (Brudvig *et al.* 1983; Styring & Rutherford 1988), where significant protein motions can still readily occur. These findings suggest that, in some S-state transitions, structural rearrangements are required for PCET to proceed and that the mechanism of PCET may not be equivalent in all S states.

Finally, modifications of the OEC, such as the depletion of Ca^{2+} or Cl^-, result in inhibition of the S-state cycle at a point where the Mn_4 cluster is in the S_2 state and Y_Z is oxidized, known as the $S_2Y_Z^{\cdot}$ state (Boussac *et al.* 1989; Hallahan *et al.* 1992; Andréasson *et al.* 1995; Szalai & Brudvig 1996; Tang *et al.* 1996*a*; Szalai *et al.* 1998*a*; Kühne *et al.* 1999; Wincencjusz *et al.* 1999). It has been suggested that the removal of these cofactors results in the disruption of the H-bonding pathways required for efficient PCET to occur (Szalai & Brudvig 1996). Spectral simulations of the EPR spectra arising from the $S_2Y_Z^{\cdot}$ state calculate an interspin distance of 7–8 Å between the Mn_4 cluster and Y_Z. This is close enough for Y_Z to be H-bonded to a water bound to Mn, either directly or via a H-bonding network involving a chain of one or more water molecules (Dorlet *et al.* 1998; Lakshmi *et al.* 1998, 1999; Peloquin *et al.* 1998; Szalai *et al.* 1998*b*).

We propose that the various observations described above can be explained by the model for PCET shown in figure 1. We distinguish between two possible types of PCET, following the convention of Cukier & Nocera (1998), as consecutive PCET or ET/PT, in which the movements of the electron and the proton are coupled but distinct events, and concerted PCET or ETPT, in which the PT and ET occur during the same event. The latter is effectively the movement of an H-atom.

The oxidation of Y_Z (figure 1*a*) involves electron transfer to $P_{680}^{+\cdot}$ and deprotonation of the phenolic proton to a basic protein residue B. Based on the mutagenesis studies described above, we identify B as H190, although it is possible that another basic residue could be the direct proton acceptor from Y_Z. BH^+ must subsequently deprotonate to dissipate the positive charge. In this regard, it has been found that the rate of proton release into the lumenal aqueous phase following photoexcitation of PSII correlates with the rate of oxidation of Y_Z (Renger & Völker 1982; Bögershausen & Junge 1995). Therefore, it appears that an efficient pathway for PT from Y_Z to the lumen must exist.

The reduction of $Y_Z^{\cdot}$, however, can proceed via two pathways. In the consecutive PCET pathway (figure 1*b*), $Y_Z^{\cdot}$ is reduced by the Mn_4 cluster and is protonated by the proton on H190 (as shown) or another basic residue B that functions as the H-bonding partner of $Y_Z^{\cdot}$. The net result is oxidation of the Mn_4 cluster by one electron. Alternatively, $Y_Z^{\cdot}$ may be both reduced and protonated by the Mn_4 cluster. In this case, an O–H bond of water ligated to Mn is broken. The net result is oxidation of the Mn_4 cluster by one electron and deprotonation of a Mn-bound water molecule via a concerted PCET reaction (figure 1*c*). The utilization of these PCET mechanisms and the switch between consecutive and concerted PCET steps during the S-state cycle are discussed in § 3.

3. PROPOSED MECHANISM FOR PHOTOSYNTHETIC WATER OXIDATION

Our proposed mechanism for photosynthetic water oxidation is depicted in figure 2. In this mechanism, a mono-oxo-bridged di-manganese unit that is proximal to Y_Z functions as the catalytic unit. Based on the oxidation state assignments for the Mn_4 cluster obtained from spectroscopic results (Yachandra *et al.* 1996), two of the four Mn ions appear to remain in the same oxidation state throughout the S-state cycle. Therefore, the remaining two Mn ions of the tetranuclear Mn cluster are denoted simply as $Mn_2^{IV}O_x$ and no direct involvement in the water oxidation chemistry is indicated. At the current 3.8 Å X-ray crystallographic resolution of PSII (Zouni *et al.* 2001), the structure and ligation of the Mn_4 cluster are unclear, although the Mn ions appear to be arranged in a compact cluster of four atoms. Such a structure is consistent with recently proposed structural models based on X-ray absorption and EPR spectroscopy (Yachandra *et al.* 1996; Peloquin *et al.* 2000). Electron paramagnetic resonance spectroscopic studies indicate that the four Mn ions are arranged in a structure with three strongly exchange-coupled Mn that are coupled more weakly to the fourth Mn. The strongly coupled Mn ions are most probably separated by 2.7 Å; two or three such Mn–Mn distances are observed in EXAFS studies and this distance is characteristic of a di-μ-oxo-bridged di-Mn unit. A longer 3.3 Å Mn–Mn distance is also observed in EXAFS studies. This distance is characteristic of a mono-μ-oxo-mono-μ-carboxylato-bridged di-Mn unit, as we propose in figure 2.

We suggest roles for D1-Asp170 and D1-His332 as manganese ligands, based on evidence from studies of site-directed mutants that these two amino acid residues are part of the OEC (Nixon & Diner 1992; Debus *et al.* 2000). The mono-oxo-bridged di-Mn unit ligated by D1-Asp170 is modelled after the active site of haemerythrin (Stenkamp *et al.* 1985), which binds O_2 reversibly. As discussed below, this structure could allow for the facile release of O_2 from the OEC in the $S_4 \rightarrow S_0$ transition. It is proposed that H332 is ligated in a trans position to the Mn ion that binds the substrate water, based on the observation that aromatic nitrogen bases trans to a metal–oxo bond enhance the reactivity of the oxo (Meunier *et al.* 1988).

As discussed in § 2 and shown in figure 1, $Y_Z^{\cdot}$ can oxidize the Mn_4 cluster by two potential mechanisms. We suggest that the sequential PCET mechanism occurs in the S-state transitions up to the S_2 state, whereas the $S_2 \rightarrow S_3$ and $S_3 \rightarrow S_4$ transitions proceed by the concerted

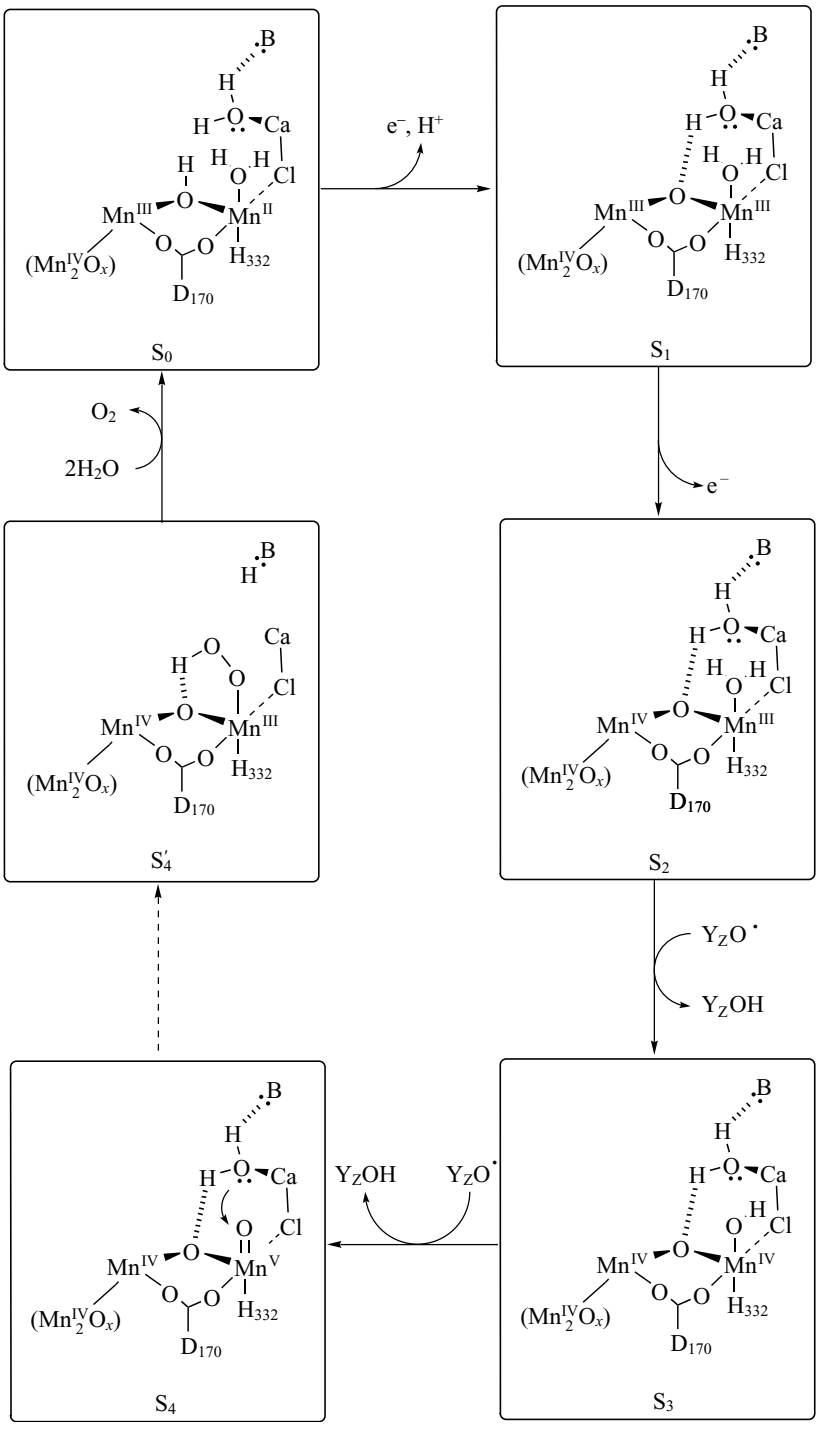

Figure 2. Proposed S-state cycle. Steps that involve H-atom abstraction by $Y_Z^{\cdot}$ from a Mn-bound water are emphasized by including the reduction of $Y_ZO^{\cdot}$ in the figure. One di-manganese unit appears not to undergo redox changes during S-state advancement and is denoted as $(Mn_2^{IV}O_x)$. B denotes a protein residue acting as a base. Adapted from Vrettos *et al.* (2001*a*).

PCET mechanism. A variety of measurements, including H/D isotope effects and temperature studies, indicate that the $S_2 \rightarrow S_3$ and $S_3 \rightarrow S_4$ transitions proceed via a different mechanism from the $S_0 \rightarrow S_1$ and $S_1 \rightarrow S_2$ transitions (reviewed in Vrettos *et al.* 2001*a*). Of particular significance is the observation that a variety of inhibitory treatments, including Ca^{2+} or Cl^- depletion and acetate or ammonia addition, cause a block beyond the $S_2Y_Z^{\cdot}$ state. We have argued that these seemingly disparate treatments could have a common effect of disrupting a H-bonding connection between $Y_Z^{\cdot}$ and a water molecule bound to Mn (Szalai & Brudvig 1996). This would prevent a concerted PCET mechanism for the oxidation of the Mn_4 cluster by $Y_Z^{\cdot}$. It has been proposed that the reactivity of metal–oxo complexes in reactions involving H-atom abstractions is determined by the energies of the O–H bonds (Mayer 1998). Based on a comparison of the measured O–H bond dissociation energies of phenols and of water bound to inorganic Mn model complexes (Bordwell & Cheng 1991; Caudle & Pecoraro 1997; Mayer 1998; Bakac 2000), H-atom abstraction by a tyrosyl radical from water bound to high-valent Mn appears

to be thermodynamically feasible. It is expected that progressive oxidations of a single tetrameric Mn cluster will occur at increasingly higher potentials, ultimately reaching a point where the thermodynamic driving force for oxidation of the Mn_4 cluster by $Y_Z^{\cdot}$ is unfavourable. We have argued that the S state transitions beyond the S_2 state are unfavourable unless the additional driving force provided by a concerted PCET mechanism is contributed. This explains why inhibitory treatments all cause a block beyond the $S_2Y_Z^{\cdot}$ state. Additionally, these observations provide evidence that only the last two S-state transitions proceed by a concerted PCET mechanism.

The $S_1 \rightarrow S_2$ transition is exceptional in that this step can occur at much lower temperatures than the other S-state transitions. It has been found that this is the only S-state transition for which no proton is released (Lavergne & Junge 1993; Kretschmann *et al.* 1996). The $S_1 \rightarrow S_2$ transition may occur via a simple outer-sphere electron transfer from the Mn_4 cluster to $Y_Z^{\cdot}$, together with the low-barrier movement of a proton from D1-His190 to $Y_Z^{\cdot}$ along a strong H-bond. Owing to the lack of proton release in the $S_1 \rightarrow S_2$ transition, this step results in a net increase in positive charge in the OEC. Consistent with this conclusion is the observation of chlorophyll absorbance band shifts that have been attributed to an electrochromic effect of the charge accumulated in the S_2 and S_3 states (Brettel *et al.* 1984; Kretschmann *et al.* 1996). We previously suggested that this charge increase is the molecular switch that causes a change from consecutive to concerted PCET mechanisms in the S-state cycle (Vrettos *et al.* 2001*a*).

Two sequential concerted PCET steps in the $S_2 \rightarrow S_3$ and $S_3 \rightarrow S_4$ transitions will lead to the formation of a Mn^V=O species, which has been proposed to be the key reactive species in O–O bond formation (Britt 1996; Hoganson & Babcock 1997; Pecoraro *et al.* 1998; Tommos *et al.* 1998; Siegbahn & Crabtree 1999; Limburg *et al.* 1999*a*). The involvement of a high-valent metal terminal–oxo species has also been postulated in homogeneous water-oxidation catalysts that generate O_2 (Gersten *et al.* 1982). Based on previous studies of metal terminal–oxo species in inorganic systems (Acquaye *et al.* 1993; Groves *et al.* 1997), it is expected that the oxo in a Mn^V=O species will be an electrophilic centre. We propose that O–O bond formation occurs in the S_4 state via nucleophilic attack on an electron-deficient Mn^V=O species by a Ca^{2+}-bound water molecule. The reactivity of the oxo may be enhanced through occupation of a Mn=O lowest unoccupied molecular orbital by a lone pair of a trans aromatic amine ligand (Jørgensen & Swanstrøm 1988). Therefore, we suggest that an imidazole moiety from a His residue (D1-His332 in our model) may be ligated in a trans position to the oxo.

O–O bond formation begins by bringing the second substrate water closer to the Mn^V=O in an S_N2-like reaction (S_4 state in figure 2). We propose that this occurs through contraction of the Mn–Cl bond upon formation of the high-valent Mn^V=O moiety. Shortening of the Mn^V–Cl bond would also increase the Lewis acidity of Ca^{2+} because of a lengthening of the Ca–Cl bond. This would have the effect of enhancing the nucleophilicity of the Ca-bound water, concomitant with formation of an electrophilic Mn^V-bound oxo. In this way, the requirement for chloride is explained in terms of both a structural role to position the Ca-bound water properly for nucleophilic attack, and as a bridge that couples the electrophilic and nucleophilic centres for reaction. In order for the O–O bond to form, there must be an overlap between the oxygen lone pair of the water molecule with an empty (non- or anti-bonding) Mn=O orbital, in accordance with Woodward–Hoffman rules of symmetry. The orientation of the Ca-bound water is optimized for a nucleophilic attack by H-bonding to the μ-oxo bridge and possibly to a Lewis base (B in figure 2); D1-H337 is one candidate for B. This base would also aid the deprotonation of water, as the pK_a of Ca-bound water (12.8 for the aqua ion; table 1) is probably too high for the Ca-bound water in PSII to be deprotonated at physiological pH.

Table 1. Ionic radii and pK_as of the aqua ions of metal cations.

metal ion	ionic radius (Å)[a]	pK_a of aqua ion[b]
Mg^{2+}	0.66	11.41
Ni^{2+}	0.69	9.86
Cu^{2+}	0.72	8.00
Co^{2+}	0.72	9.85
Cd^{2+}	0.97	9.00
Ca^{2+}	0.99	12.80
Sr^{2+}	1.12	13.18
Ba^{2+}	1.34	13.36
Lu^{3+}	0.85	7.94
Dy^{3+}	0.91	8.10
Gd^{3+}	0.92	9.78
Pr^{3+}	1.01	8.91
La^{3+}	1.02	8.82
Na^{+}	0.97	14.77
K^{+}	1.33	16
Cs^{+}	1.67	>17

[a] Data from Weast (1978).
[b] Data from Dean (1985).

Nucleophilic attack by the Ca-bound water on the Mn^V=O moiety, concomitant with its deprotonation, results in a transiently formed hydroperoxide species (denoted S_4' in figure 2), in which the OOH moiety is H-bonded to the bridging μ-oxo. This structure is analogous to that of reversibly bound O_2 in haemerythrin (Stenkamp *et al.* 1985; Holmes *et al.* 1991). The active site of haemerythrin consists of an Fe^{II} dimer connected by a mono-μ-hydroxo-di-μ-carboxylato bridge. Oxygen binds as a hydroperoxide by oxidizing the dimer to Fe_2^{III} and deprotonating the μ-OH to a μ-O; the proton remains H-bonded to the bridging μ-O. The Fe^{III} ions are separated by 3.3 Å with an Fe–O–Fe angle of 125°. The release of O_2 is simply the reverse of its binding, in which the proton is transferred back to the μ-O and the Fe dimer is reduced to the diferrous state. By analogy, release of O_2 from the OEC is proposed to proceed by a similar mechanism. In haemerythrin, reversible O_2 binding is allowed energetically because the reduction potentials for the Fe_2^{II}/Fe_2^{III} couple in haemerythrin (Armstrong *et al.* 1983) and HOO^-/O_2 couple (Wood 1988) are nearly equal, at *ca.* 500 mV. However, in the case of the Mn_4 cluster, the reduction potential for the S_0 state is substantially higher than that of hydroperoxide, so oxidation of hydroperoxide is energetically favoured. The reduction of the terminal

Mn^{III}–OOH to Mn^{II} results in the release of O_2 and the protonation of the μ-oxo bridge, resetting the OEC to S_0.

4. THE ROLE OF CALCIUM IN THE O_2-EVOLVING COMPLEX

One prediction of the model shown in figure 2 is that Ca^{2+} functions as a Lewis acid in the OEC. In order to test this idea, we have studied the binding of a series of cations to the Ca^{2+} site in PSII (Vrettos *et al.* 2001*b*).

Previous studies of Ca^{2+}-binding sites in other proteins have defined two general types of sites (reviewed in Falke *et al.* 1994). Charge-selective sites exhibit a shallow dependence of the binding free energy (ΔG_B) on the ionic radius of the cation for a given charge, but a significant difference in ΔG_B between cations of different charges (figure 3*a*). However, size-selective sites exhibit a potential well with a well-defined minimum at the optimal ionic radius, but have similar optimal ΔG_B values for di- and trivalent cations (figure 3*b*). The difference can be understood in terms of the rigidity of the binding site. Charge-selective sites typically coordinate a small number of amino acid ligands to the metal centre, leaving several waters of hydration on the metal. Selectivity is governed solely by neutralization of the net negative charge of the binding cavity by the metal ion. By employing many amino acid ligands and allowing fewer (typically only one) water ligands to remain on the metal ion, size-selective sites are, however, significantly more rigid. Selectivity is governed by size according to the extent to which the net negative charge density of the binding cavity is neutralized by the metal ion. For this reason, trivalent cations show a slightly smaller optimal radius than dications due to their greater net positive charge density, which can contract the ligand sphere more tightly (figure 3*b*). In the case of size-selective sites, work must be done to expand the binding cavity to accommodate ions larger than the optimal radius. The steepness of the potential well at radii greater than the optimal radius is a measure of this work, which reflects the constraining force of the site.

Data for the Ca^{2+}-binding site in PSII clearly indicate that the site is rigid (figure 3*c*). The constraining energy of the Ca^{2+}-binding site in PSII is 17 kcal mol^{-1}, similar to that measured for EF-hand-like sites (Falke *et al.* 1994). The site in PSII is, therefore, highly optimized to bind metal ions of a particular size. By analogy with other size-selective Ca^{2+}-binding proteins, this suggests that the Ca^{2+}-binding site in PSII consists of an ordered closely packed array of mostly carboxylate oxygen ligands. One difference between the Ca^{2+}-binding site in PSII and EF-hand-like sites is that there is little distinction between di- and trivalent cations (compare figure 3*b* and 3*c*). It is possible that the trivalent ions, which are strong Lewis acids, bind to PSII with a hydroxide ligand and so have a net +2 charge upon binding. This has previously been proposed to account for structural effects on the Mn_4 cluster induced by substituting Dy^{3+} for Ca^{2+} (Riggs-Gelasco *et al.* 1996). Another difference between PSII and EF-hand-like sites is the presence of polarizable groups in the OEC (such as the Mn_4 cluster) that can alter the electrical effects of the nearby amino acid ligands by dissipating some of the net negative charge.

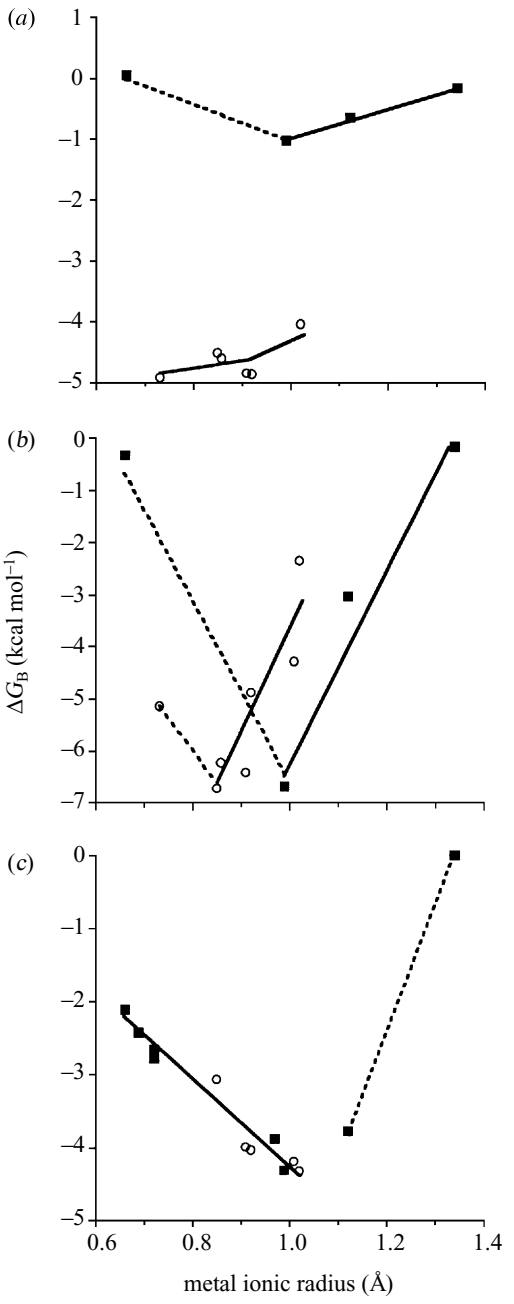

Figure 3. K_D of divalent (squares) and trivalent (open circles) metal ions binding to Ca^{2+}-binding sites versus their ionic radius for (*a*) a charge-selective EF-hand-like site; (*b*) a size-selective EF-hand-like site; and (*c*) the Ca^{2+}-binding site in PSII membranes. Schemes (*a*,*b*) adapted from Falke *et al.* (1991) and scheme (*c*) adapted from Vrettos *et al.* (2001*b*).

Considering the large number of metal ions that will compete for the Ca^{2+}-binding site in PSII, it is surprising that only Ca^{2+} and Sr^{2+} support O_2 evolution. It would be expected that if the role of Ca^{2+} in PSII is purely structural, then metal ions of the same size and charge should be functional replacements. For example, Cd^{2+} (0.97 Å) is almost the same size as Ca^{2+} (0.99 Å), carries the same charge, is a closed-shell ion and binds to PSII with an affinity that is comparable with that of Ca^{2+}. Moreover, Cd^{2+} replaces Ca^{2+} in other proteins without large structural perturbations and even preserves H-bonding networks (McPhalen *et al.* 1991; Bouckaert *et al.* 2000). However, Cd^{2+}-substituted PSII is inactive. What is the

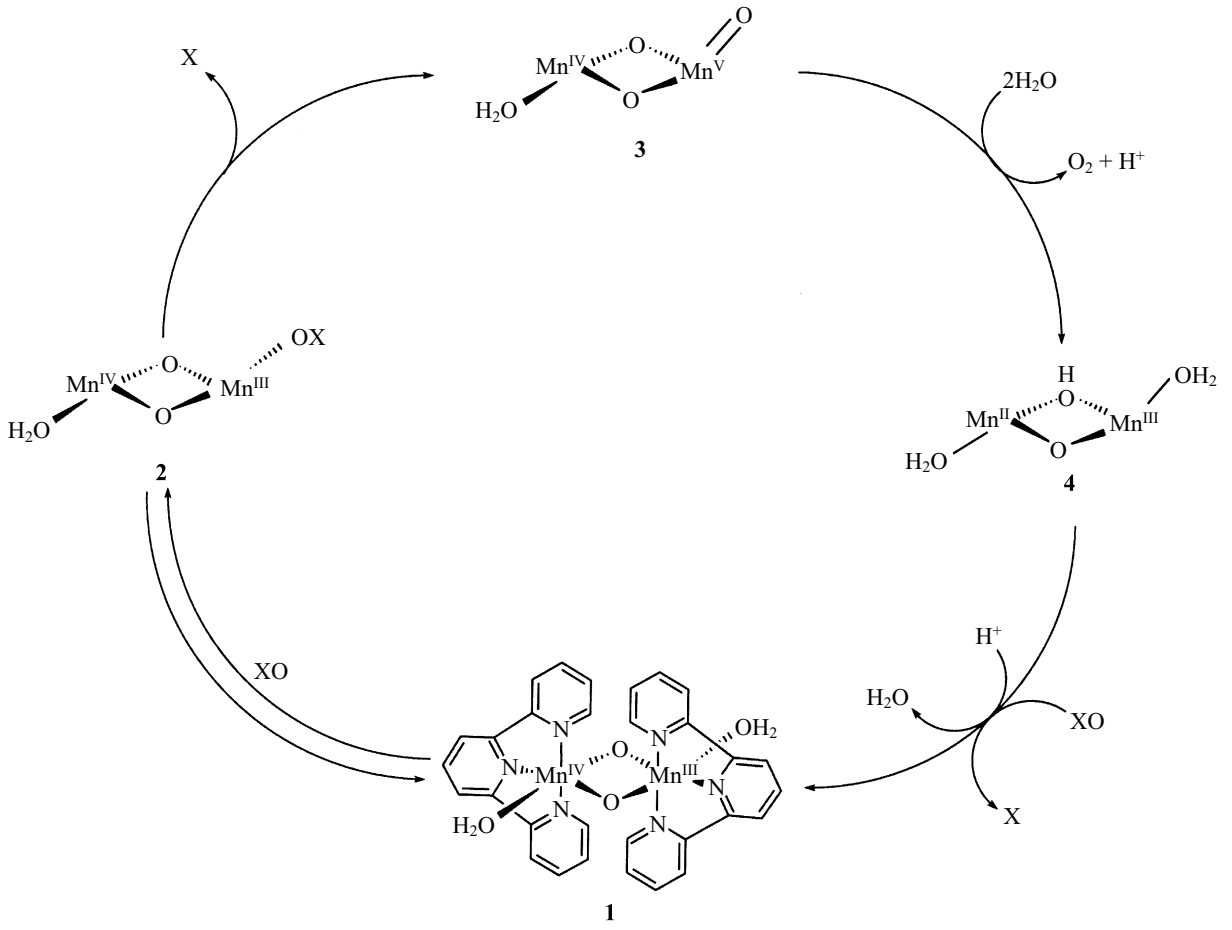

Figure 4. Proposed mechanism for the reaction between **1** and oxygen atom-transfer reagents. Adapted from Limburg *et al.* (2001).

distinguishing factor among the metal ions that determines the functional competence of Ca^{2+} and Sr^{2+} over other cations that can bind in the Ca^{2+}-binding site in PSII? Values of ionic radii and pK_as of the aqua ions are shown in table 1. Owing to its larger size, Sr^{2+} is not a particularly good match to the size of the Ca^{2+}-binding site in PSII and does not bind to PSII as tightly as Ca^{2+} (Vrettos et al. 2001*b*). However, among the cations that can bind with reasonable affinity to the Ca^{2+} binding site in PSII, only Sr^{2+} has a pK_a of its aqua ion that is close to that of Ca^{2+}. We postulate that only Sr^{2+} can functionally substitute for Ca^{2+} because it is the only cation whose Lewis acidity is well matched. Other metal ions fail to support oxygen evolution because their Lewis acidity is too far out of the range required for activity, which makes the coordinated water too strong (or weak) a Brønsted acid. The result is that the H-bonding network of the OEC is disturbed and the coordinated water either deprotonates to form an unreactive metal cation-bound OH^- (too strong a Brønsted acid) or cannot be readily deprotonated in the O–O bond-forming reaction (too weak a Brønsted acid).

There are two possibilities for the protonation state of the Ca^{2+}-bound water: either OH^- or H_2O. When buried in the hydrophobic interior of a protein, the pK_a of water bound to a metal ion is usually lowered by several units; nonetheless, the relative ordering of the Lewis acidity of the metal ions in table 1 will remain the same. Taking this into consideration, the Ca^{2+} aqua ion is still a weak Lewis acid (pK_a = 12.8) compared with the other metal ions in table 1, so we propose that H_2O, and not OH^-, is the form of the Ca^{2+}-bound substrate molecule. Sr^{2+} is the only other catalytically competent metal ion because its pK_a is sufficiently high to provide H_2O and not OH^- as a ligand.

These results suggest that Ca^{2+} is directly involved in the chemistry of water oxidation and is not just a structural cofactor in the OEC. They provide good support for our proposal that the function of Ca^{2+} is to act as a Lewis acid, binding a substrate water molecule and tuning its reactivity.

5. CATALYSIS OF O–O BOND FORMATION BY INORGANIC MANGANESE COMPLEXES

A Mn^{V}=O species is proposed to be the key reactive species in O–O bond formation in the mechanism outlined in figure 2 (Vrettos *et al.* 2001*a*) and in a number of other proposals (Britt 1996; Hoganson & Babcock 1997; Pecoraro *et al.* 1998; Tommos *et al.* 1998; Siegbahn & Crabtree 1999; Limburg *et al.* 1999*a*). In order to probe the chemistry of high-valent manganese terminal-oxo species, we have studied the reaction of inorganic manganese complexes with oxygen atom-transfer reagents such as potassium oxone ($KHSO_5$) and sodium hypochlorite (NaOCl) (Limburg *et al.* 1997, 1999*b*, 2001).

We found that the addition of $KHSO_5$ or NaOCl to an aqueous solution of **1** ([(terpy)$(H_2O)Mn^{III}(O)_2Mn^{IV}$

(OH_2)(terpy)](NO$_3$)$_3$ (terpy=2,2′-6,2″-terpyridine); figure 4) resulted in the catalytic formation of O_2 (Limburg *et al.* 1997, 1999*b*, 2001). These are, to our knowledge, the first reports of a di-μ-oxo dimanganese complex, a structural element of the Mn_4 cluster in the OEC, which can carry out catalytic O–O bond formation. The reactions followed Michaelis–Menten kinetics with V_{max} values of 2420 for $KHSO_5$ at pH 4.5 and 6.5 for NaOCl at pH 8.6 in units of mol O_2 (mol **1**)$^{-1}$ h^{-1}. The observations that the reactions are first-order with respect to **1** and show saturation kinetics are consistent with a mechanism that involves initial binding of the oxygen atom-transfer reagent (termed XO) followed by a rate-determining step leading to O_2 formation. In order to investigate the mechanism further, we performed isotope-labelling studies. By carrying out the reaction in ^{18}O-labelled water using ^{16}O-labelled oxone, it was possible to determine the source of the oxygen atoms in the product O_2. It was found that significant amounts of both singly and doubly ^{18}O-labelled O_2 were formed, indicating that the reaction must involve a reactive intermediate containing an active oxygen that can exchange rapidly with water. The incorporation of ^{18}O from water into various organic products has been used to infer the presence of a Mn=O intermediate in other systems (Groves & Stern 1987, 1988; Bernadou *et al.* 1994; Groves *et al.* 1997; Bernadou & Meunier 1998). On this basis, we concluded that a Mn^V=O species is the reactive intermediate in the O_2-evolving reaction catalysed by **1**. Figure 4 summarizes the proposed mechanism for the reaction between **1** and oxygen atom-transfer reagents.

These results provide support for the formation of a reactive high-valent manganese intermediate in the reaction of **1** with oxygen atom-transfer reagents. We propose that the active intermediate contains a Mn^V=O species that is capable of reacting with water to produce O_2. Studies are in progress to characterize further the mechanisms of O_2 formation in both our model system and PSII. A key aim of our model studies is to characterize the reactive intermediates that are present during catalysis. These species may be analogous to those formed in the OEC during turnover and thus their characterization will provide important insights into the mechanism of photosynthetic water oxidation.

This work was supported by the National Institutes of Health (GM32715).

REFERENCES

Acquaye, J. H., Muller, J. G. & Takeuchi, K. J. 1993 Oxidation of thioanisoles and methyl phenyl sulfides by oxo(phosphine)ruthenium(IV) complexes. *Inorg. Chem.* **32**, 160–165.

Andréasson, L.-E., Vass, I. & Styring, S. 1995 Ca^{2+} depletion modifies the electron transfer on both donor and acceptor sides in photosystem II from spinach. *Biochim. Biophys. Acta* **1230**, 155–164.

Armstrong, F. A., Harrington, P. C. & Wilkins, R. G. 1983 Reduction potentials of various haemerythrin oxidation states. *J. Inorg. Biochem.* **18**, 83–91.

Bakac, A. 2000 Hydrogen atom abstraction by metal–oxo and metal–superoxo complexes: kinetics and thermodynamics. *J. Am. Chem. Soc.* **122**, 1092–1097.

Bernadou, J. & Meunier, B. 1998 'Oxo-hydroxo tautomerism' as a useful mechanistic tool in oxygenations catalysed by water soluble metalloporphyrins. *J. Chem. Soc. Chem. Comm.* 2167–2173.

Bernadou, J., Fabiano, A.-S., Robert, A. & Meunier, B. 1994 'Redox tautomerism' in high-valent metal–oxo–aqua complexes. Origin of oxygen atom in epoxidation reactions catalysed by water-soluble metalloporphyrins. *J. Am. Chem. Soc.* **116**, 9375–9376.

Berthomieu, C., Hienerwadel, R., Boussac, A., Breton, J. & Diner, B. A. 1998 Hydrogen bonding of redox-active tyrosine Z of photosystem II probed by FTIR difference spectroscopy. *Biochemistry* **37**, 10 547–10 554.

Bögershausen, O. & Junge, W. 1995 Rapid proton-transfer under flashing light at both functional sides of dark-adapted photosystem II particles. *Biochim. Biophys. Acta* **1230**, 177–185.

Bögershausen, O., Haumann, M. & Junge, W. 1996 Photosynthetic oxygen evolution: H/D isotope effects and the coupling between electron and proton transfer during transitions $S_2 \rightarrow S_3$ and $S_3 \rightarrow S_4 \rightarrow S_0$. *Ber. Bunsenges. Phys. Chem.* **100**, 1987–1992.

Bordwell, F. G. & Cheng, J.-P. 1991 Substituent effects on the stabilities of phenoxyl radicals and the acidities of phenoxyl radical cations. *J. Am. Chem. Soc.* **113**, 1736–1743.

Bouckaert, J., Loris, R. & Wyns, L. 2000 Zinc/calcium- and cadmium/cadmium-substituted concanavalin A: interplay of metal binding, pH and molecular packing. *Acta Cryst.* D **56**, 1569–1576.

Boussac, A., Zimmermann, J.-L. & Rutherford, A. W. 1989 EPR signals from modified charge accumulation states of the oxygen evolving enzyme in Ca^{2+}-deficient photosystem II. *Biochemistry* **28**, 8984–8989.

Brettel, K., Schlodder, E. & Witt, H. T. 1984 Nanosecond reduction kinetics of photooxidized chlorophyll a-II (P-680) in single flashes as a probe for the electron pathway, H^+-release and charge accumulation in the O_2-evolving complex. *Biochim. Biophys. Acta* **766**, 403–415.

Britt, R. D. 1996 Oxygen evolution. In *Oxygenic photosynthesis: the light reactions*, vol. 4 (ed. D. R. Ort & C. F. Yocum), pp. 137–159. Dordrecht, The Netherlands: Kluwer.

Brudvig, G. W., Casey, J. L. & Sauer, K. 1983 The effect of temperature on the formation and decay of the multiline EPR signal species associated with photosynthetic oxygen evolution. *Biochim. Biophys. Acta* **723**, 366–371.

Casey, J. L. & Sauer, K. 1984 Electron paramagnetic resonance detection of a cryogenically photogenerated intermediate in photosynthetic oxygen evolution. *Biochim. Biophys. Acta* **767**, 21–28.

Caudle, M. T. & Pecoraro, V. L. 1997 Thermodynamic viability of hydrogen atom transfer from water coordinated to the oxygen-evolving complex of photosystem II. *J. Am. Chem. Soc.* **119**, 3415–3416.

Christen, G. & Renger, G. 1999 The role of hydrogen bonds for the multiphasic $P680^{+\cdot}$ reduction by Y_Z in photosystem II with intact oxygen evolution capacity. Analysis of kinetic H/D isotope exchange effects. *Biochemistry* **38**, 2068–2077.

Christen, G., Seeliger, A. & Renger, G. 1999 $P680^{+\cdot}$ reduction kinetics and redox transition probability of the water oxidizing complex as a function of pH and H/D isotope exchange in spinach thylakoids. *Biochemistry* **38**, 6082–6092.

Chu, H.-A., Nguyen, A.-P. & Debus, R. J. 1995*a* Amino acid residues that influence the binding of manganese or calcium to photosystem II. 1. The lumenal interhelical domains of the D1 polypeptide. *Biochemistry* **34**, 5839–5858.

Chu, H.-A., Nguyen, A.-P. & Debus, R. J. 1995*b* Amino acid residues that influence the binding of manganese or calcium to photosystem II. 2. The carboxy-terminal domain of the D1 polypeptide. *Biochemistry* **34**, 5859–5882.

Cukier, R. I. & Nocera, D. G. 1998 Proton-coupled electron transfer. *A. Rev. Phys. Chem.* **49**, 337–369.

Dean, J. A. 1985 *Lange's handbook of chemistry*, 13th edn. New York: McGraw-Hill.

Debus, R. J. 1992 The manganese and calcium ions of photosynthetic oxygen evolution. *Biochim. Biophys. Acta* **1102**, 269–352.

Debus, R. J., Campbell, K. A., Peloquin, J. M., Pham, D. P. & Britt, R. D. 2000 Histidine 332 of the D1 polypeptide modulates the magnetic and redox properties of the manganese cluster and tyrosine Y_Z in photosystem II. *Biochemistry* **39**, 470–478.

Diner, B. A., Force, D. A., Randall, D. W. & Britt, R. D. 1998 Hydrogen bonding, solvent exchange, and coupled proton and electron transfer in the oxidation and reduction of redox-active tyrosine Y_Z in Mn-depleted core complexes of photosystem II. *Biochemistry* **37**, 17 931–17 943.

Dorlet, P., Di Valentin, M., Babcock, G. T. & McCracken, J. L. 1998 Interaction of $Y_Z^{\cdot}$ with its environment in acetate-treated photosystem II membranes and reaction center cores. *J. Phys. Chem.* B **102**, 8239–8247.

Falke, J. J., Snyder, E. E., Thatcher, K. C. & Voertler, C. S. 1991 Quantitating and engineering the ion specificity of an EF-hand-like Ca^{2+} binding site. *Biochemistry* **30**, 8690–8697.

Falke, J. J., Drake, S. K., Hazard, A. L. & Peersen, O. B. 1994 Molecular tuning of ion binding to calcium signaling proteins. *Q. Rev. Biophys.* **27**, 219–290.

Gersten, S. W., Samuels, G. J. & Meyer, T. J. 1982 Catalytic oxidation of water by an oxo-bridged ruthenium dimer. *J. Am. Chem. Soc.* **104**, 4029–4030.

Ghanotakis, D. F., Babcock, G. T. & Yocum, C. F. 1984 Calcium reconstitutes high rates of oxygen evolution in polypeptide depleted photosystem II preparations. *FEBS Lett.* **167**, 127–130.

Groves, J. T. & Stern, M. K. 1987 Olefin epoxidation by manganese(IV) porphyrins: evidence for two reaction pathways. *J. Am. Chem. Soc.* **109**, 3812–3814.

Groves, J. T. & Stern, M. K. 1988 Synthesis, characterization, and reactivity of oxomanganese(IV) porphyrin complexes. *J. Am. Chem. Soc.* **110**, 8628–8638.

Groves, J. T., Lee, J. & Marla, S. S. 1997 Detection and characterization of an oxomanganese(V) porphyrin complex by rapid-mixing stopped-flow spectrophotometry. *J. Am. Chem. Soc.* **119**, 6269–6273.

Hallahan, B. J., Nugent, J. H. A., Warden, J. T. & Evans, M. C. W. 1992 Investigation of the origin of the 'S3' EPR signal from the oxygen-evolving complex of photosystem 2: the role of tyrosine Z^{+}. *Biochemistry* **31**, 4562–4573.

Haumann, M., Bögershausen, O., Cherepanov, D., Ahlbrink, R. & Junge, W. 1997 Photosynthetic oxygen evolution: H/D isotope effects and the coupling between electron and proton transfer during the redox reactions at the oxidizing side of photosystem II. *Photosynth. Res.* **51**, 193–208.

Hays, A.-M. A., Vassiliev, I. R., Golbeck, J. H. & Debus, R. J. 1998 Role of D1-His190 in proton-coupled electron transfer reactions in photosystem II: a chemical complementation study. *Biochemistry* **37**, 11 352–11 365.

Hays, A.-M. A., Vassiliev, I. R., Golbeck, J. H. & Debus, R. J. 1999 Role of D1-His190 in the proton-coupled oxidation of tyrosine Y_Z in manganese-depleted photosystem II. *Biochemistry* **38**, 11 851–11 864.

Hoganson, C. W. & Babcock, G. T. 1997 A metalloradical mechanism for the generation of oxygen from water in photosynthesis. *Science* **277**, 1953–1956.

Holmes, M. A., Le Trong, I., Turley, S., Sieker, L. C. & Stenkamp, R. E. 1991 Structures of deoxy and oxy haemerythrin at 2.0 Å resolution. *J. Mol. Biol.* **218**, 583–593.

Joliot, P. & Kok, B. 1975 Oxygen evolution in photosynthesis. In *Bioenergetics of photosynthesis* (ed. Govindjee), pp. 387–412. New York: Academic.

Jørgensen, K. A. & Swanstrøm, P. 1988 On the proximal effect of the nitrogen ligands on the oxomanganese porphyrin system. *Acta Chem. Scand.* **43**, 822–824.

Karge, M., Irrgang, K.-D. & Renger, G. 1997 Analysis of the reaction coordinate of photosynthetic water oxidation by kinetic measurements of 355 nm absorption changes at different temperatures in photosystem II preparations suspended in either H_2O or D_2O. *Biochemistry* **36**, 8904–8913.

Koike, H., Hanssum, B., Inoue, Y. & Renger, G. 1987 Temperature dependence of S-state transition in a thermophilic cyanobacterium, *Synechococcus vulcanus* Copeland measured by absorption changes in the ultraviolet region. *Biochim. Biophys. Acta* **893**, 524–533.

Kok, B., Forbush, B. & McGloin, M. 1970 Cooperation of charges in photosynthetic O_2 evolution. I. A linear four step mechanism. *Photochem. Photobiol.* **11**, 457–475.

Kretschmann, H., Schlodder, E. & Witt, H. T. 1996 Net charge oscillation and proton release during water oxidation in photosynthesis. An electrochromic band shift study at pH 5.5–7.0. *Biochim. Biophys. Acta* **1274**, 1–8.

Kühne, H. & Brudvig, G. W. 2002 Proton-coupled electron transfer involving tyrosine Z in photosystem II. *J. Phys. Chem.* B **106**, 8189–8196.

Kühne, H., Szalai, V. A. & Brudvig, G. W. 1999 Competitive binding of chloride and acetate in photosystem II. *Biochemistry* **38**, 6604–6613.

Lakshmi, K. V., Eaton, S. S., Eaton, G. R., Frank, H. A. & Brudvig, G. W. 1998 Analysis of dipolar and exchange interactions between manganese and tyrosine Z in the $S_2Y_Z^{\cdot}$ state of acetate-inhibited photosystem II via spectral simulations at X- and Q-bands. *J. Phys. Chem.* B **102**, 8327–8335.

Lakshmi, K. V., Eaton, S. S., Eaton, G. R. & Brudvig, G. W. 1999 Orientation of the tetranuclear manganese cluster and tyrosine Z in the O_2-evolving complex of photosystem II: an EPR study of the $S_2Y_Z^{\cdot}$ state in oriented acetate-inhibited photosystem II membranes. *Biochemistry* **38**, 12 758–12 767.

Lavergne, J. & Junge, W. 1993 Proton release during the redox cycle of the water oxidase. *Photosynth. Res.* **38**, 279–296.

Limburg, J., Brudvig, G. W. & Crabtree, R. H. 1997 O_2 evolution and permanganate formation from high-valent manganese complexes. *J. Am. Chem. Soc.* **119**, 2761–2762.

Limburg, J., Szalai, V. A. & Brudvig, G. W. 1999*a* A mechanistic and structural model for the formation and reactivity of a Mn^{V}=O species in photosynthetic water oxidation. *J. Chem. Soc. Dalton Trans.* 1353–1363.

Limburg, J., Vrettos, J. S., Liable-Sands, L. M., Rheingold, A. L., Crabtree, R. H. & Brudvig, G. W. 1999*b* A functional model for O–O bond formation by the O_2-evolving complex in photosystem II. *Science* **283**, 1524–1527.

Limburg, J., Vrettos, J. S., Chen, H., de Paula, J. C., Crabtree, R. H. & Brudvig, G. W. 2001 Characterization of the O_2-evolving reaction catalyzed by $[(terpy)(H_2O)Mn^{III}(O)_2Mn^{IV}(OH_2)(terpy)](NO_3)_3$ (terpy=2,2′-6,2″-terpyridine). *J. Am. Chem. Soc.* **123**, 423–430.

McPhalen, C. A., Strynadka, N. C. J. & James, M. N. G. 1991 Calcium-binding sites in proteins: a structural perspective. *Adv. Protein Chem.* **42**, 77–144.

Mamedov, F., Sayre, R. T. & Styring, S. 1998 Involvement of histidine 190 on the D1 protein in electron/proton transfer reactions on the donor side of photosystem II. *Biochemistry* **37**, 14 245–14 256.

Mayer, J. M. 1998 Hydrogen atom abstraction by metal–oxo complexes: understanding the analogy with organic radical reactions. *Accts Chem. Res.* **31**, 441–450.

Meunier, B., Decarvalho, M. E., Bortolini, O. & Momenteau, M. 1988 Proximal effect of the nitrogen ligands in the cata-

lytic epoxidation of olefins by the NaOCl/manganese(III) porphyrin system. *Inorg. Chem.* **27**, 161–164.
Michel, H. & Deisenhofer, J. 1988 Relevance of the photosynthetic reaction center from purple bacteria to the structure of photosystem II. *Biochemistry* **27**, 1–7.
Nixon, P. J. & Diner, B. A. 1992 Aspartate 170 of the photosystem II reaction center polypeptide D1 is involved in the assembly of the oxygen-evolving manganese cluster. *Biochemistry* **31**, 942–948.
Noguchi, T., Inoue, Y. & Tang, X.-S. 1997 Structural coupling between the oxygen-evolving Mn cluster and a tyrosine residue in photosystem II as revealed by Fourier transform infrared spectroscopy. *Biochemistry* **36**, 14 705–14 711.
Ono, T. & Inoue, Y. 1984 Ca^{2+}-dependent restoration of O_2-evolving activity in $CaCl_2$-washed PS II particles depleted of 33, 24 and 16 kDa proteins. *FEBS Lett.* **168**, 281–286.
Pecoraro, V. L., Baldwin, M. J., Caudle, M. T., Hsieh, W.-Y. & Law, N. A. 1998 A proposal for water oxidation in photosystem II. *Pure Appl. Chem.* **70**, 925–929.
Peloquin, J. M., Campbell, K. A. & Britt, R. D. 1998 ^{55}Mn pulsed ENDOR demonstrates that the photosystem II 'split' EPR signal arises from a magnetically-coupled mangano–tyrosyl complex. *J. Am. Chem. Soc.* **120**, 6840–6841.
Peloquin, J. M., Campbell, K. A., Randall, D. W., Evanchik, M. A., Pecoraro, V. L., Armstrong, W. H. & Britt, R. D. 2000 ^{55}Mn ENDOR of the S_2-state multiline EPR signal of photosystem II: implications on the structure of the tetranuclear Mn cluster. *J. Am. Chem. Soc.* **122**, 10 926–10 942.
Rappaport, F. & Lavergne, J. 1997 Charge recombination and proton transfer in manganese-depleted photosystem II. *Biochemistry* **36**, 15 294–15 302.
Renger, G. & Völker, M. 1982 Studies on the proton release pattern of the donor side of system 2. Correlation between oxidation and deprotonization of donor D1 in tris-washed inside-out thylakoids. *FEBS Lett.* **149**, 203–207.
Riggs-Gelasco, P. J., Mei, R., Ghanotakis, D. F., Yocum, C. F. & Penner-Hahn, J. E. 1996 X-ray absorption spectroscopy of calcium-substituted derivatives of the oxygen-evolving complex of photosystem II. *J. Am. Chem. Soc.* **118**, 2400–2410.
Rutherford, A. W., Zimmermann, J.-L. & Boussac, A. 1992 Oxygen evolution. In *The photosystems: structure, function and molecular biology* (ed. J. Barber), pp. 179–229. Amsterdam: Elsevier.
Siegbahn, P. E. M. & Crabtree, R. H. 1999 Manganese oxyl radical intermediates and O–O bond formation in photosynthetic oxygen evolution and a proposed role for the calcium cofactor in photosystem II. *J. Am. Chem. Soc.* **121**, 117–127.
Stenkamp, R. E., Sieker, L. C., Jensen, L. H., McCallum, J. D. & Sanders-Loehr, J. 1985 Active site structures of deoxyhaemerythrin and oxyhaemerythrin. *Proc. Natl Acad. Sci. USA* **82**, 713–716.
Styring, S. & Rutherford, A. W. 1988 Deactivation kinetics and temperature dependence of the S-state transitions in the oxygen-evolving system of photosystem II measured by EPR spectroscopy. *Biochim. Biophys. Acta* **933**, 378–387.
Szalai, V. A. & Brudvig, G. W. 1996 Reversible binding of nitric oxide to tyrosyl radicals in photosystem II. Nitric oxide quenches formation of the S3 EPR signal species in acetate-inhibited photosystem II. *Biochemistry* **35**, 15 080–15 087.
Szalai, V. A., Kühne, H., Lakshmi, K. V. & Brudvig, G. W. 1998*a* Characterization of the interaction between manganese and tyrosine Z in acetate-inhibited photosystem II. *Biochemistry* **37**, 13 594–13 603.
Szalai, V. A., Stone, D. A. & Brudvig, G. W. 1998*b* A structural and mechanistic model of the O_2-evolving complex of photosystem II. In *Photosynthesis: mechanisms and effects* (ed. G. Garab), pp. 1403–1406. Dordrecht, The Netherlands: Kluwer.
Tang, X.-S., Randall, D. W., Force, D. A., Diner, B. A. & Britt, R. D. 1996*a* Manganese–tyrosine interaction in the photosystem II oxygen-evolving complex. *J. Am. Chem. Soc.* **118**, 7638–7639.
Tang, X.-S., Zheng, M., Chisholm, D. A., Dismukes, G. C. & Diner, B. A. 1996*b* Investigation of the differences in the local protein environments surrounding tyrosine radicals $Y_Z^{\cdot}$ and $Y_D^{\cdot}$ in photosystem II using wild-type and the D2-Tyr1-60Phe mutant of *Synechocystis* 6803. *Biochemistry* **35**, 1475–1484.
Tommos, C., Tang, X.-S., Warncke, K., Hoganson, C. W., Styring, S., McCracken, J., Diner, B. A. & Babcock, G. T. 1995 Spin-density distribution, conformation, and hydrogen bonding of the redox-active tyrosine Y_Z in photosystem II from multiple electron paramagnetic-resonance spectroscopies: implications for photosynthetic oxygen evolution. *J. Am. Chem. Soc.* **117**, 10 325–10 335.
Tommos, C., Hoganson, C. W., Di Valentin, M., Lydakis-Simantiris, N., Dorlet, P., Westphal, K., Chu, H.-A., McCracken, J. & Babcock, G. T. 1998 Manganese and tyrosyl radical function in photosynthetic oxygen evolution. *Curr. Opin. Chem. Biol.* **2**, 244–252.
Vrettos, J. S., Limburg, J. & Brudvig, G. W. 2001*a* Mechanism of photosynthetic water oxidation: combining biophysical studies of photosystem II with inorganic model chemistry. *Biochim. Biophys. Acta* **1503**, 229–245.
Vrettos, J. S., Stone, D. A. & Brudvig, G. W. 2001*b* Quantifying the ion selectivity of the Ca^{2+} site in photosystem II: evidence for direct involvement of Ca^{2+} in O_2 formation. *Biochemistry* **40**, 7937–7945.
Weast, R. C. 1978 *CRC handbook of chemistry and physics*, 59th edn. West Palm Beach, FL: CRC Press.
Wincencjusz, H., van Gorkom, H. J. & Yocum, C. F. 1997 The photosynthetic oxygen-evolving complex requires chloride for its redox state $S_2 \rightarrow S_3$ and $S_3 \rightarrow S_0$ transitions but not for $S_0 \rightarrow S_1$ or $S_1 \rightarrow S_2$ transitions. *Biochemistry* **36**, 3663–3670.
Wincencjusz, H., Yocum, C. F. & van Gorkom, H. J. 1999 Activating anions that replace Cl^- in the O_2-evolving complex of photosystem II slow the kinetics of the terminal step in water oxidation and destabilize the S_2 and S_3 states. *Biochemistry* **38**, 3719–3725.
Wood, P. M. 1988 The potential diagram for oxygen at pH 7. *Biochem. J.* **253**, 287–289.
Yachandra, V. K., Sauer, K. & Klein, M. P. 1996 Manganese cluster in photosynthesis: where plants oxidize water to dioxygen. *Chem. Rev.* **96**, 2927–2950.
Zouni, A., Witt, H. T., Kern, J., Fromme, P., Krauß, N., Saenger, W. & Orth, P. 2001 Crystal structure of photosystem II from *Synechococcus elongatus* at 3.8 Å resolution. *Nature* **409**, 739–743.

Discussion

C. Dismukes (*Department of Chemistry, Princeton University, Princeton, NJ, USA*). Your model requires a short distance (less than 4 Å) with the Y_Z directly attacking the water bound to the Mn^{IV}-OH_2? The recent XRD model indicates that this distance is no closer than 7.5 Å.

G. W. Brudvig. Assuming that the identification of Y_Z and the structure of the Mn_4 cluster in the XRD model are correct, then the distance between the two is 7.5 Å. This distance is too long for a direct H-bond between Y_Z and H_2O bound to a terminal Mn. However, protons from a Mn-bound H_2O can still be transferred to $Y_Z^{\cdot}$ through an intervening H-bond pathway, such as via an ordered chain of H_2O molecules.

L. Hammarström (*Department of Physical Chemistry, Uppsala University, Uppsala, Lund, Sweden*). Are the kinetic results that you presented in terms of Michaelis–Menten parameters (the difference between oxone and hypochlorite) consistent with the mechanistic model?

G. W. Brudvig. The different Michaelis–Menten parameters measured for oxone versus hypochlorite reflect the chemical differences between the two oxidants. A direct comparison of the K_M values is, however, complicated by the different pH values (8.6 for OCl^- versus 4.5 for HSO_5^-) at which the measurements were done. On the other hand, the V_{max} for oxone is 400 times greater than for OCl^-. This makes sense because oxone is a stronger oxidant that OCl^- and SO_4^{2-} is a better leaving group than Cl^- for forming the terminal-oxo species.

W. Junge (*Abteilung Physik, Universität Osnabrück, Osnabrück, Germany*). You mention that strontium can replace calcium by virtue of its Lewis basicity. What about barium, which has a similar basicity?

G. W. Brudvig. Although barium has a similar basicity to calcium, it is a non-competitive inhibitor, which means that it inhibits O_2 evolution not by binding to the Ca^{2+}-binding site but in some other way. Therefore, even though Ba^{2+} meets the chemical criteria for replacing Ca^{2+}, it does not bind to the Ca^{2+}-binding site in the OEC.

P. E. M. Siegbahn (*Department of Physics, University of Stockholm, Stockholm, Sweden*). I wonder if your assignment of the active species in water oxidation as Mn^{V}=O could be taken literally? A Mn^{IV}-oxygen radical is the precursor for di-oxygen formation. In fact, even in your $(Mn)_2$ dimer model system we find this oxygen radical. Furthermore, in our studies of di-oxygen cleavage in different enzymes like Mn catalase, phenylalanine hydroxylase, methane mono-oxygenase and cytochrome oxidase, we find that oxygen radicals appear directly after di-oxygen cleavage.

G. W. Brudvig. The electronic state of the reactive Mn-oxo species, i.e. Mn^{V}=O versus Mn^{IV}–$O^{\cdot}$, does not affect the proposed mechanism. However, further work is needed to determine the nature of the species that is the precursor for O_2 formation.

P. E. M. Siegbahn. A second question, I wonder about your structural model for the S_2 to S_3 transition. I do not see how your model could account for the large structural rearrangement indicated by EXAFS.

G. W. Brudvig. It should be noted that a consensus has not been reached on the interpretation of the EXAFS data for the $S_2 \rightarrow S_3$ transition. In any case, our model does not explicitly include the structure of two of the four Mn ions in the Mn_4 cluster or any of their ligands. Therefore, changes in those structures can account for the structural perturbations measured by EXAFS in the $S_2 \rightarrow S_3$ transition.

J. De Las Rivas (*Instituto de Microbiología y Bioquímica, Universidad de Salamanca, Salamanca, Spain*). You said that PSII has a Ca^{2+}-binding site that seems to be size-selective and rigid. Have you found any protein motif that could be a candidate to give structure to this binding site? Which proteins could be involved in the formation of such a binding site: D1 extrinsic loops, PsbO….?

G. W. Brudvig. Ca^{2+}-binding sites are generally composed of an array of electron-rich O-donor ligands, such as Glu and Asp residues, peptide backbone carbonyls and water. Therefore, any protein fold that offers such an array is a candidate for the Ca^{2+}-binding site, making it difficult to assign possible motifs from the PSII sequence. It is likely that the 17 and 23 kDa polypeptides can be excluded as ligand donors, however, because Ca^{2+} still binds tightly in their absence.

J. De Las Rivas. Regarding the ions that can substitute Ca(II), you said that the only one is Sr. What about Mg? There is a report in the literature by Enami *et al.* (1995) that in red algae and cyanobacteria, Mg^{2+} can restore activity in Ca-depleted PSII. These authors say that this restoration does not occur in higher plants.

G. W. Brudvig. The competitive binding of Ca^{2+} with other metal cations has not been explored in great detail in cyanobacteria and red algae. It may be that Mg^{2+}, which is smaller than Ca^{2+} but almost as basic, is able to bind to the Ca^{2+} site in red algae and cyanobacteria sufficiently well that it can support O_2 evolution. This would support our hypothesis that it is the basicity of the metal ion in the Ca^{2+} site that determines functionality.

Additional reference

Enami, I., Murayama, H., Onta, H., Kamo, M., Nakazato, K. & Shen, J. R. 1995 Isolation and characterization of a photosystem II complex from the red alga *Cyanidium caldarium*: association of cytochrome *c*-550 and 12 kDA protein with the complex. *Biochim. Biophys. Acta* **1232**, 208–216.

GLOSSARY

EPR: electron paramagnetic resonance
ET: electron transfer
EXAFS: extended X-ray absorption fine structure
OEC: oxygen-evolving complex
PCET: proton-coupled electron transfer
PSII: photosystem II
PT: proton transfer
XRD: X-ray diffraction